Coherent sea level fluctuations along the global continental slope

By Chris W. Hughes and Michael P. Meredith

Proudman Oceanographic Laboratory, Liverpool, U.K.

Signals in sea level or, more properly, sub-surface pressure (SSP; sea level corrected for the inverse barometer effect) are expected to propagate rapidly along the continental slope due to the effect of sloping topography on wave modes, resulting in strongly correlated SSP over long distances. Observations of such correlations around the Arctic and Antarctic are briefly reviewed, and then extended using satellite altimetry to the rest of the global continental slope. It is shown that such long-distance correlations are common, especially in extra-tropical regions. Simple correlations from altimetry cannot, however, establish the wave speed, or whether waves are responsible for the correlations as opposed to large-scale coherence in the forcing. A case study around South America is used to highlight some of the complications, and is found to strengthen the case for the importance of wave modes in such long-distance SSP coherence, although more detailed in-situ data are required to resolve the cause of the correlations.

Keywords: Sea Level, Continental Slope, Kelvin Waves

1. Introduction

Advection apart, there are two ways for information about changes in forcing to propagate across an ocean basin. It can propagate roughly westwards across the ocean interior as a Rossby wave signal (or eastwards as a Kelvin wave at the equator), or it can propagate around the boundary. For a vertical sidewall with stratification, the boundary waves are baroclinic Kelvin waves, whereas for a sloping sidewall without stratification they are barotropic continental shelf waves, or topographic Rossby waves. In reality, boundary waves are a hybrid of the two types (Huthnance, 1978), resembling Kelvin waves more as the stratification increases. Over long distances, friction is also expected to become important, although its effect can be counterintuitive. While, in some circumstances, friction simply damps the waves and limits the distance over which they can propagate, or allows deep ocean sea level signals to propagate across the slope and onto the shelf (Huthnance, 2004), Clarke and Van Gorder (1994) argue that, at long periods, it is possible for friction to act so as to trap a sea level signal at the coast where it would otherwise be expected to radiate to the west as a Rossby wave.

Such boundary waves propagate along the continental slope, the effective boundary of the deep ocean. In principle, their signal should usually be detectable on the shelf, however local wind-driven dynamics can often dominate (especially on the larger shelf regions) and act to mask the signal. It is perhaps for this reason, and because the Pacific signal is large due to signals associated with El Niño, that the

only really convincing tide gauge based evidence for long-distance propagation of signals along the coast has come from the west coast of North and South America (Enfield and Allen, 1980), where the continental shelf is very narrow. These waves typically travel at speeds ranging from about 1 ms^{-1} near the equator to 2–3 ms^{-1} at higher latitudes (Enfield and Allen, 1980; Meyers et al., 1998), although even faster speeds are expected in places (for example, Cartwright et al. (1980) calculate a shelf wave speed of 4.5 ms^{-1} for the K_1 tide on the Hebrides Shelf). They are forced by a combination of equatorial sea level anomalies propagating polewards, of which the most energetic waves can reach as far north as Alaska (Meyers et al., 1998), plus longshore wind stress, which usually becomes dominant at higher latitudes (Enfield and Allen, 1980). The waves are thought to start near the equator with a Kelvin wave-like structure, and evolve towards a continental shelf wave structure at higher latitudes (Suginohara, 1981). More recent studies with satellite altimetry show the waves propagating at least as far south as 40°S, and radiating Rossby waves into the ocean interior (e.g. Vega et al., 2003).

With such rapid propagation speeds, the most obvious observable effect of these waves is a smoothing of the sea level signal over large distances along the continental slope. To be more precise, it is not sea level which is smoothed, but sub-surface pressure (SSP)—sea level after correction for an inverse-barometer response to atmospheric pressure. Even given the long and well-resolved time series from tide gauges along the west coast of the American continent, it is difficult to accurately determine wave propagation speeds, due to the presence of background "noise" and forcing which may itself have long length scales (Meyers et al., 1998; Chelton and Davis, 1982).

Large scale coherence of sea level signals has also been identified from tide gauges and altimetry around the Antarctic continent (Aoki, 2002; Hughes et al., 2003), although propagation of the signal cannot be clearly identified. In this case the forcing is clearly related to a recognised circumpolar mode of the atmospheric circulation, the Southern Annular Mode or Antarctic Oscillation. This relationship is clearly illustrated in Figure 1, which shows the correlation of atmospheric pressure with a 10-year record of ocean bottom pressure from the south side of Drake Passage (see Hughes et al., 2003; Meredith et al., 2004 for details). Atmospheric pressure is from the National Centers for Environmental Prediction (NCEP) reanalysis project (Kalnay et al., 1996), obtained from *http://www.cdc.noaa.gov/cdc/reanalysis/reanalysis.shtml*, and time series have been filtered to pass periods of 30–170 days for which the ocean dynamics are most clearly understood. Hughes et al. (2003) and Meredith et al. (2004) demonstrated a correlation between the BPR and tide gauge data and the Antarctic Oscillation, showing that the Antarctic Oscillation forces a circumpolar mode in the ocean. Here we see the other side of the picture: the atmospheric mode forcing the BPR data is clearly circumpolar, with strongest positive correlation near to Antarctica, and a weaker negative correlation in subtropical latitudes, which corresponds to the surface pressure manifestation of the Antarctic Oscillation.

The aim of this paper is to see whether coherent sea level signals can be seen in other parts of the global continental slope, using satellite altimetry. We are guided in this aim by the observation that there is often a minimum in variance of sea level and/or a phase change in the seasonal cycle in sea level at the continental slope as seen in altimetry (Jakobsen et al., 2003, for example), suggesting that sea level at

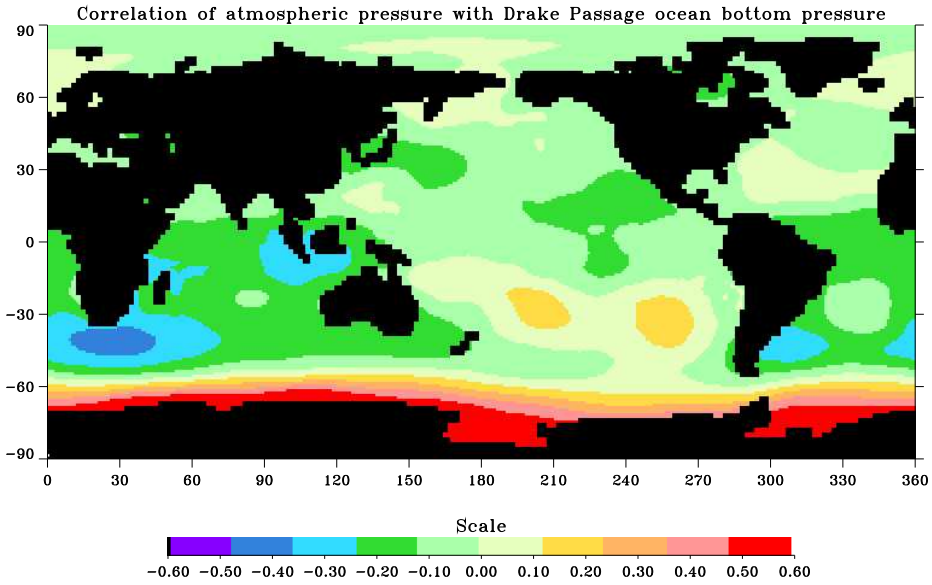

Figure 1. Correlation of ocean bottom pressure from 1000m depth at the south side of Drake Passage with surface atmospheric pressure from the NCEP reanalysis data. Both time series have been filtered to pass periods of 30–170 days. The strong positive correlation around Antarctica and weaker negative correlation around the Subtropics denote forcing by the Antarctic Oscillation

the slope is not dominated by either deep ocean eddies or by shallow water storm surge dynamics, and may therefore be the best place to look for relatively small amplitude but long length scale coherent sea level changes.

Around Antarctica, the presence of sea ice makes it difficult to study this mode of variability using satellite altimetry, as a very small fraction of the area of coherent SSP variability is not covered by ice at some point in the year. However, even here, it is possible to demonstrate the circumpolar coherence from altimetry. Figure 2 (upper panel) shows the coherent mode as it was initially identified in the Fine Resolution Antarctic Model as a mode associated with fluctuations in the transport around Antarctica (Hughes et al., 1999). This panel first appeared as Fig. 11 in Woodworth et al. (1996). The lower panel shows the correlation of SSP from altimetry with that averaged over the Weddell Sea region marked by the box (topography is contoured for reference); this is the main region of the coherent mode where altimetric SSP can be extracted without too much data loss due to sea ice. Correlation is weaker in the case of altimetry (lower panel), as might be expected due to the more complicated processes occuring in the real ocean compared with the model, and due to noise in the altimeter measurement (a typical root-mean-square variability in SSP is less than 5 mbar, or 2.6 mbar for the Weddell Sea average, making it comparable to the expected noise in altimeter measurements). Even so, the patterns are remarkably similar, even down to such features as a small tongue of higher correlation up the eastern side of the Kerguelan Plateau at about 85°E (the northern part of the model is less reliable due to its limited domain, which

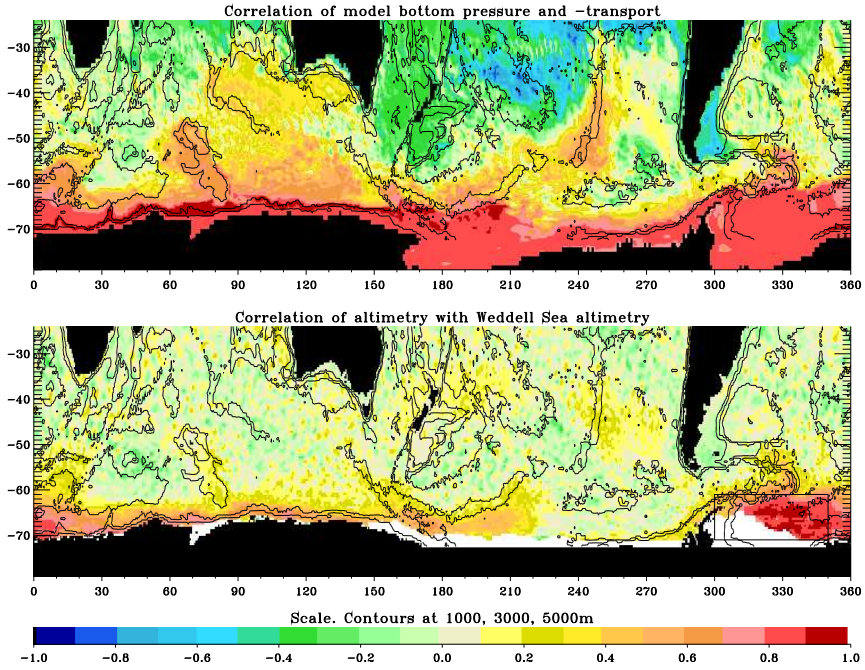

Figure 2. Plots of (top) correlation of SSP in the Fine Resolution Antarctic Model with model transport around Antarctica, and (bottom) correlation of SSP from altimetry with SSP averaged over the Weddell Sea region shown by a box. Depth contours 5000 m, 3000 m, and 1000 m are in black. White represents regions with too little useable altimetry data.

ends at 24°S). The model prediction of coherence in this region is therefore clearly vindicated, although it should be noted that statistical significance is difficult to demonstrate in this case as the seasonal cycle of sea ice cover makes it hard to assess the impact of the seasonal cycle on the correlation coefficient. We must instead appeal to the heuristic justification that the band of higher than 'background' correlation is spatially well-correlated with that expected from the model.

A second place where coherence has recently been predicted by model results is the Arctic (Hughes and Stepanov, 2003). Whilst this prediction has some support from tide gauge data, the completely pan-Arctic nature of the correlation is yet to be established as the available tide gauge data are almost all from the Russian and Scandinavian continental shelf. Conventional altimetry data are of little use in this region, again because of sea ice.

Given the success of altimetry even in a region of small signal and intermittent ice cover, and the apparent ubiquity of coherence at high latitudes, a natural extension is to use altimetry to look for coherence along continental slopes around the world. In order to attempt this, we have extracted sea level data from the gridded combined altimeter product produced by the ENACT project (Ducet et al, 2000; available from ftp://ftp.cls.fr/pub/oceano/enact/msla) along the global continental slope. This product is produced by mapping sea level anomalies from a combina-

tion of Topex/Poseidon, Jason, ERS, and Envisat altimetry, assuming a correlation function which drops to zero at 300 km at the equator, reducing to 80 km at 80 degrees N or S. The effective resolution is therefore somewhere between this scale and the altimeter track separation which is 0.72 degrees of longitude for the ERS data (35 day repeat), and 2.83 degrees for Topex/Poseidon and Jason (9.92 day repeat). Past studies such as Hughes and Ash (2001) have found that the mapped product is better than considering individual tracks for studies of mesoscale processes, as it uses the full dataset efficiently and reduces orbit errors.

2. The Global Continental Slope

In order to define a vector of grid points which correspond to the global continental slope, the bathymetry of Smith and Sandwell (1997) was first averaged onto the same 1/3 degree Mercator grid on which the altimeter data are provided. A geographically-varying depth was then subjectively chosen to mark the continental slope, and a contour-following algorithm used to identify grid points along this contour. This produced an ordered list of 4042 grid points plotted in Figure 3, along with a plot of depth versus grid point number. Grid point zero is at the southern tip of South Africa, with every tenth grid point plotted as a large spot in Figure 3, and every hundredth grid point numbered.

The varying depth was chosen so as to follow the steep part of the continental slope without being diverted into complex island regions or semi-enclosed seas, and without extending away from the continental slope into the deep ocean. It was found to be impossible to achieve this with a single depth. The depth is 1500m from Spain, around Africa and past India. It then deepens to 1900m to avoid entering the complex Indonesian region. At the southern tip of Australia it deepens further to 2400m to avoid Indonesia from the other side. There is a brief shallowing to 1000m near Japan to avoid a diversion along the relatively shallow Sitito-Iozima Ridge, returning to 2400m as far as Pacific Central America, where a shallowing to 1200m is necessary to avoid following the ridge system to the Galapagos Islands. A further shallowing to 650m is needed just before Florida Strait in order to pass through the strait rather than around the Caribbean islands, followed by a slight deepening to 800m near to Iceland to avoid entering the Arctic region. The depth finally reverts to 1500m near to Spain.

The SSP was then extracted from the altimetry maps at these points, and annual and semiannual terms were removed by least squares fitting. The top panel of Figure 4 shows the resulting time series. Interannual signals are dominated by the influence of El Niño in the equatorial Pacific and Indian Oceans, and some slowly-propagating short wavelength features can be made out (more clearly in magnified views). There are also horizontal stripes clearly visible, particularly in the North Atlantic and parts of the Pacific, denoting large-scale coherence of SSP along the continental slope. In order to concentrate on these features, the data were filtered further to remove periods longer than one year, and spatial smoothing was performed using a running mean of 100 grid points along the continental slope; the resulting time series are plotted in the lower panel of Figure 4.

It is immediately apparent that coherent signals occur across long distances, especially in the North Pacific and North Atlantic (note however that the use of a Mercator grid means that the spacing between grid points is greater near the equa-

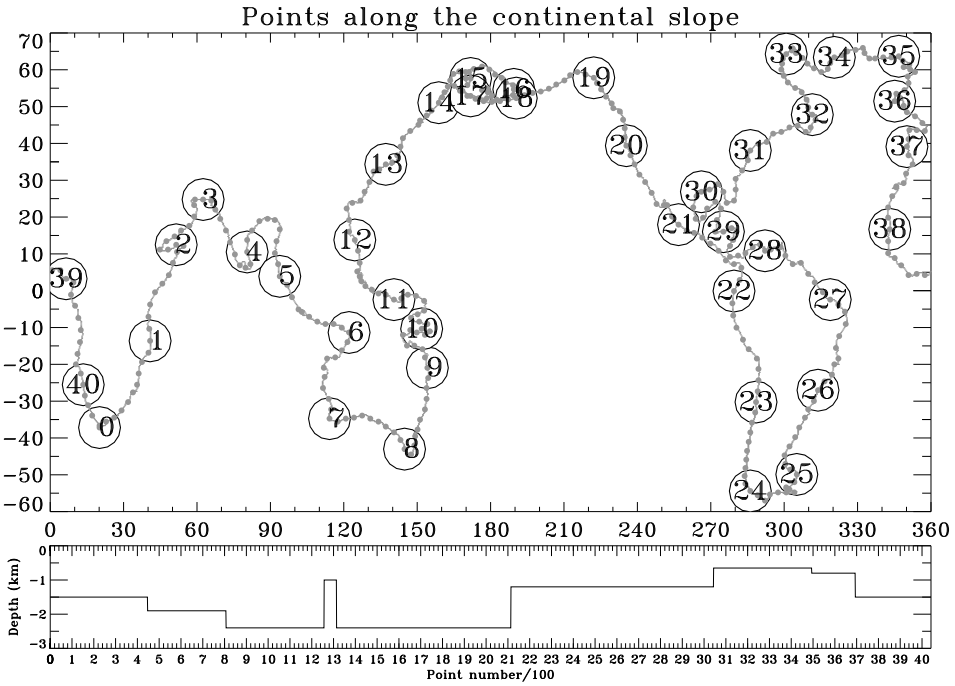

Figure 3. Map showing positions of grid points chosen to represent the continental slope. Every tenth grid point is marked with a grey spot, and every hundredth gridpoint is numbered. At the bottom is plotted the depth at these grid points, as a function of grid point number divided by 100.

tor than at high latitudes). In order to objectively quantify this, cross-correlations at zero lag were calculated between time series constructed by high pass filtering in time as above, and averaging over independent sections of 100 grid points (giving 41 time series including one at the end which covers only 42 grid points), or 50 grid points (giving 81 time series including one at the end which covers only 42 grid points). The distance corresponding to 100 grid points varies depending on both latitude and orientation of the slope, but is typically 4000–5000 km near the equator, and half that at latitude 60°. No special consideration is given to the equator in forming these averages, as early investigations considering each basin separately (and adding sea level along the equator) did not show any special behaviour or discontinuities at the equator. The cross-correlations are all plotted in Figure 5, with 50-grid point averages above the diagonal and 100-grid point averages below the diagonal.

In order to assess significance levels, a Monte Carlo error analysis was performed. Strictly, such an analysis should be performed for each pair of time series correlated but, given the number of pairs both here and in the maps considered later, such an approach is impractical. Instead, we calculated a typical power spectrum, and a standard deviation of that power spectrum, by first normalising the (unfiltered) time series to unit power, calculating the fourier transform, and averaging across the 41 or 81 different time series (both were tried, with very little difference). The resulting spectrum is presented in variance preserving form in Figure 6. A

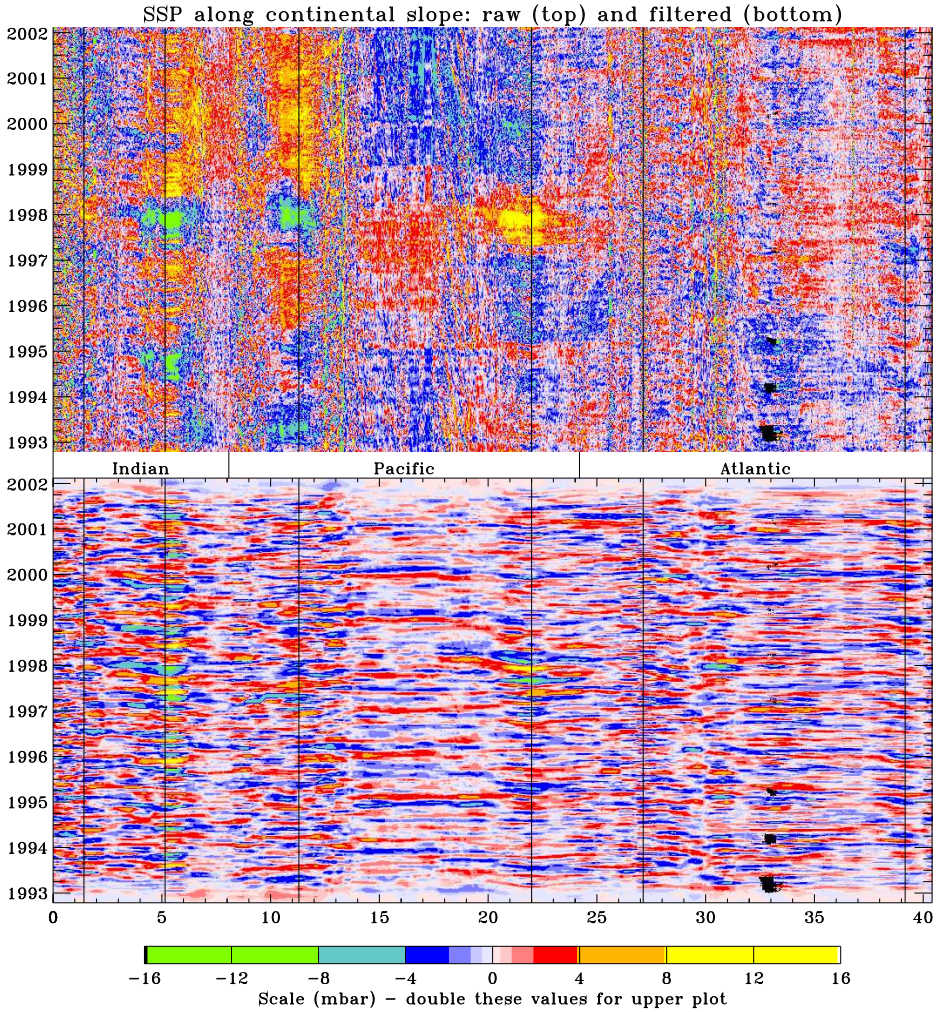

Figure 4. Plot of sub-surface pressure as a function of time and grid point number along the continental slope. Black lines mark equator crossings, other black is missing data due to sea ice. The annual and semiannual cycles have been removed (top), and (bottom) periods longer than 1 year have been filtered out, and a running average of 100 grid points taken

series of 200 random time series was produced, each of which had the same power spectrum plus random perturbations within the calculated standard deviation, and random phase for the fourier components. These were each then filtered in the same way as the real data. All possible cross correlations were calculated, giving 40,000 values, which were then sorted. Significance levels were calculated by two methods: simply counting the value of correlation coefficient below which 95% or 99% of the randomly generated values fell, and fitting a curve based on the expectations for a χ^2 distribution for n degrees of freedom, performing a nonlinear fit to calculate the best value of n (the curves fitted this distribution well). Both methods yielded

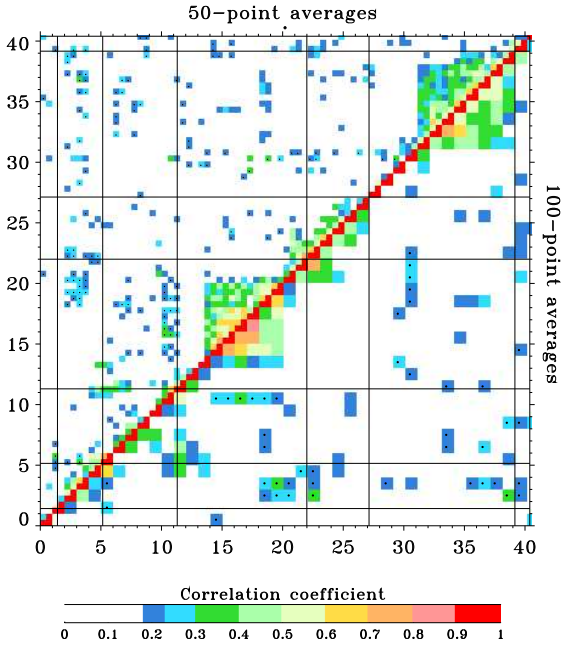

Figure 5. Correlation coefficients between pairs of averaged sea level time series. Sea level averaged over 50 grid points above the diagonal, 100 grid points below. Negative values are marked with a black dot and black lines denote equator crossings. Correlations above 0.18 are significant at the 95% level, with lower values left white. Correlations between 0.18 and 0.23 (the 99% significance level) are dark blue. Squares of high correlation denote regions of strong coherence of SSP along the continental slope, especially the North and Central Pacific (13.5-20; 20-24), South America (23-27) and the North Atlantic (31-39).

values of 0.18 for 95% confidence, and 0.23 for 99% confidence, with a variation of ± 0.01 for different methods and for the difference between 41 and 81 time series. These values are used in all subsequent plots.

The regions of strong correlation are clear here as squares of high correlation. The squares encompass points 13.5–20 (North Pacific), 20–24 (Central Pacific), 23–27 (South America), and 31-39 (North Atlantic). Elsewhere there are often correlations over distances of about 100 grid points, but rarely more. An exception is the section 11–12 on Figure 3 which correlates significantly with all points from 4 to 13, except the section 8–9 where the East Australian Current introduces extra variability. This appears to be due to a combination of correlations along the continental slope, and through the islands separating the Indian and Pacific oceans.

The Central Pacific square, centred on point 22, has a sharp cut-off to the north at about point 20.5. This corresponds to the region around Baja California where the continental slope has a complicated shape, potentially acting as a barrier to wave propagation, although the strongest equatorial events associated with El Niño certainly propagate further north than this, sometimes reaching Alaska as found by Meyers et al. (1998). To the south, the Central Pacific square merges with a South American square, which clearly shows correlations between the eastern and

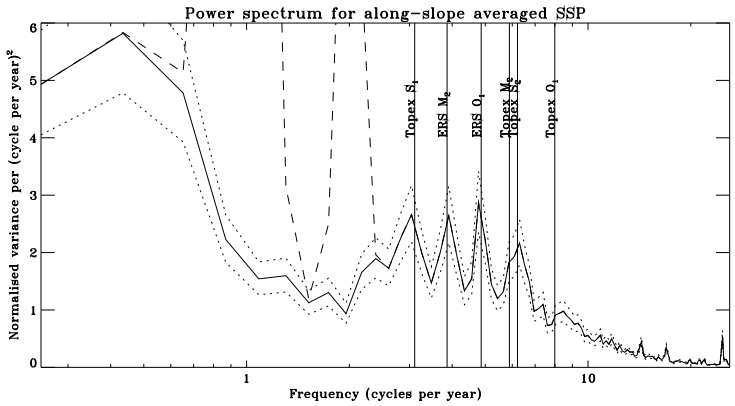

Figure 6. Average power spectrum from the 41 along-slope averaged sea level time series, after each has been normalized to unit power. The dashed line shows the average of the time series with no filtering. The solid line is from the time series with only annual and semiannual cycles subtracted and the dotted line shows one sample standard deviation above and below this. Aliased frequencies of the dominant semidiurnal and diurnal tides as sampled by the satellites involved are marked as vertical lines.

western continental slopes of South America. This will be discussed in more detail in the next section.

The North Pacific and North Atlantic squares have a sharp cut off at about points 13.5 and 31 respectively, close to the separation points of the Kuroshio and Gulf Stream. Correlations of these modes with NCEP reanalysis wind stress each show significant but rather weak correlations with a gyre pattern of wind stress, centred on 41°N, 19°W in the Atlantic and on about 35°N in the Pacific (not shown). These patterns are consistent with what would be expected as a coastal sea level response to longshore winds, but also serve to emphasise how difficult it is to distinguish the effects of wave propagation from those due to large-scale coherence in forcing.

An immediate question concerns the subjective nature of the choice of depth contour. A full investigation of the impact of this is difficult, although some alternatives have been explored (such as choosing a contour which does not enter the Caribbean Sea, or a constant depth for the whole of the western Americas). In general we find that the coherent signals occur where the slope is steep and well-defined, so that a choice of different depths does not move the chosen position horizontally very far, so the significant correlations seem quite robust (although there must remain some uncertainty concerning the possibility of short cross-slope length scales in the signal). What is less clear is whether the negative results (no significant correlation) could be the result of choosing the 'wrong' contour. There is no evidence of this from the investigations we have performed so far. Neither path around the Caribbean shows significant correlation with regions to the north or south, and the reduced correlation between points north and south of Baja California appears to be genuine and due to the complex and changing slope topography in that region, rather than being associated with a change in contour depth. None of the other sudden changes in correlation is associated with a depth change.

A second question concerns possible errors due to inadequate removal of tidal signals from the data, a particular concern close to the coast. The main diurnal and semidiurnal tides alias to a variety of frequencies which depend on the satellite repeat period. The major aliased frequencies in the band of interest are marked on Figure 6. It is clear that some tidal signal is leaking through, but that it accounts for less than a third of the variance in this band. Importantly though, the altimetry samples tidal phase in a very complicated manner, with nearby tracks typically producing large phase differences. The combination of data from two different altimeters will increase this tendency, resulting in tidal errors typically having short length scales. We would not, therefore expect along-slope correlations to be the result of tidal errors, even if the tides are coherent over long distances. The possibility of 'accidental' correlations, simply because the time series have spectral peaks at the same frequencies due to tidal errors, is accounted for by the Monte Carlo error analysis.

3. Case Studies

To look in more detail at the causes of these correlations, we concentrate next on two particular regions: we first make some comments on the North Atlantic mode, before discussing in more detail the South American mode.

Correlations along the slope may be due to signals which are confined to the slope, or they may be simply due to basin-scale modes being sampled at the slope. To distinguish between these possibilities, the time series averaged along several short sections of slope have been extracted. These time series were then correlated with time series of sea level from every point in the world. Two example results are shown in Fig. 7, in which the short section of slope from which the original time series was taken is marked by a series of black dots. These clearly demonstrate that the coherence is predominantly along the slope. The North Atlantic coherence stretches from the Tropics on the African side to beyond the Grand Banks on the west, following the continental slope and also extending north along the Norwegian continental slope. This mode appears to be similar to that recently discussed by Skagseth (2004), with a similar relationship to the wind stress, and suggests that the signal identified by Skagseth is not limited to the eastern side of the Atlantic, but also influences the western side at least as far as the Scotia shelf. This contrasts with the results of Orvik and Skagseth (2003), who show that interannual variations in the northward flow in the Norwegian Atlantic Slope Current are predicted by wind stress curl at 55°N, with a 15 month lag. No such lag is seen in the higher frequency signals investigated here. Note how, in many places, the significant correlation does not extend close to the shore, suggesting that the coherent mode may be difficult to detect with tide gauges.

The South American segment in Figure 7 shows that part of the signal along the southern Chile continental slope originates at the equator, resulting in correlations north of the equator as the same signal propagates away from the equator in both directions. This is one region where the direction of propagation can be unambiguously determined, from tide gauges (Enfield and Allen, 1980) or from altimetry (Vega et al., 2003). Altimetry also shows the subsequent radiation of Rossby waves into the Pacific interior at interannual periods (lagged correlations also suggest this at the shorter periods considered here, but the Rossby waves are

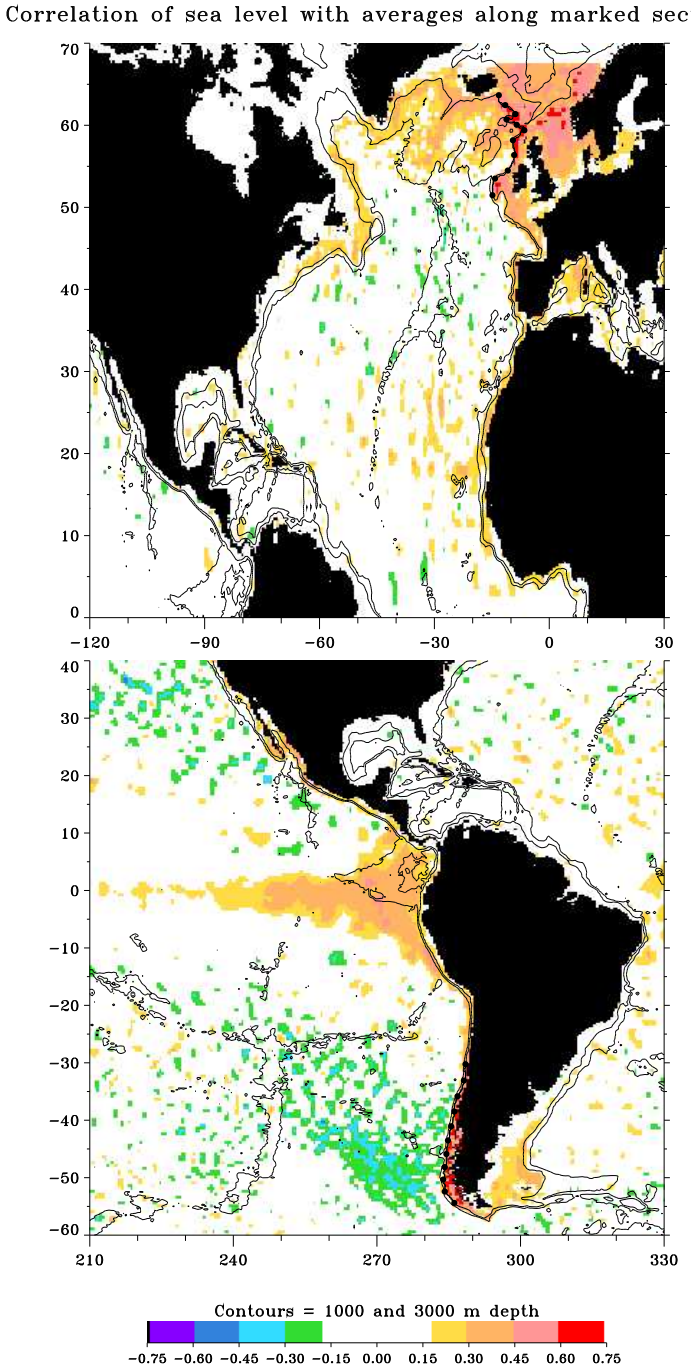

Figure 7. Correlation of sub-surface pressure at each grid point, with sub-surface pressure averaged along the sections marked with black dots in each panel. Correlations smaller than 0.18 are not significant at the 95% level and are left white. For 99% significance the correlation coefficient must be 0.23 or above. Depth contours at 1000 and 3000 m are also shown.

confined to a region closer to the equator). We here see that the signal from the equator reaches all the way to the southern tip of South America, and that part of the signal observed off Chile also propagates up the other side of the continent. This is also demonstrated by Figure 5, which shows significant correlation between SSP averages 23–23.5 and 25-25.5, as well as 24–24.5 and 26–26.5. It is worth noting that this is a rapidly-propagating, long wavelength signal, as opposed to the slower, short wavelength features which have previously been noted propagating in parts of this region (Johnson, 1990). Further evidence of this is shown in Woodworth et al. (2004), where it is demonstrated that tide gauge measurements from Port Stanley (Falkland Islands) are sensitive with minimal lag to large-scale winds over the eastern equatorial Pacific.

There are indications of a negative correlation offshore, at around 40–50°S, which appears to be connected with the topography of the Chile Rise. This raises questions concerning the spatial structure of the associated wave modes. Suginohara (1981) first noted that waves starting as baroclinic Kelvin waves near the Pacific equator would evolve into barotropic continental shelf waves at higher latitudes, as the stratification weakens. This has the effect that the initially horizontal node in the Kelvin wave mode tilts upwards to become a vertical node, meaning that positive and negative pressure anomalies are separated laterally, rather than vertically as in the Kelvin wave. An anticorrelation offshore is then what would be expected, although the presence of the Chile Rise appears to have distorted this.

Further circumstantial evidence for a node in the structure of the signal can be seen from in-situ data. The Proudman Oceanographic Laboratory has measured ocean bottom pressure in Drake Passage since 1988 (e.g. Meredith et al., 1996). In particular, there are almost complete records from the northern side of the passage for the period 28 November 1988 to 20 July 1992, at site FS1 (53.54°S, 57.02°W, at 2800 m depth) and for the period 16 November 1992 to 21 December 1997 at site ND2 (54.94°S, 58.39°W, at 1000 m depth). These two positions are marked as black spots in Figure 8. Unfortunately, the timeseries do not overlap, making a direct comparison impossible, but comparison with the NCEP reanalysis winds suggests that the two sites may be measuring similar signals with opposite phase, suggesting the presence of a node somewhere between the 1000 m and the 2800 m isobaths. This is illustrated in Fig. 8, which shows as vectors the complex correlation coefficient between winds and bottom pressure. This is the correlation between bottom pressure (a scalar) and the two-dimensional vector wind stress treated as a complec number. All time series here were band-pass filtered for the period range 30–170 days, in order to retain most of the period range of interest while minimizing contamination due to the annual redeployment of the bottom pressure recorders. The patterns in the two cases are very similar (though not completely identical), with correlation with winds that are to the east or southeast over the northern part of the eastern South Pacific, and which then turn southwards along the South American coast, as would be expected for a raising of sea level at the coast. Note, however, that the sign of the correlation with FS1 (the deeper instrument) has been reversed in this picture. The correlations therefore suggest a reversed response to winds at 2800 m, as compared with 1000 m depth. It is impossible to tell, however, whether this is due to a horizontal node separating shallow from deep flows, a vertical node separating flows in the horizontal, or something intermediate between these cases. Correlations between altimetry and either winds or bottom pressure

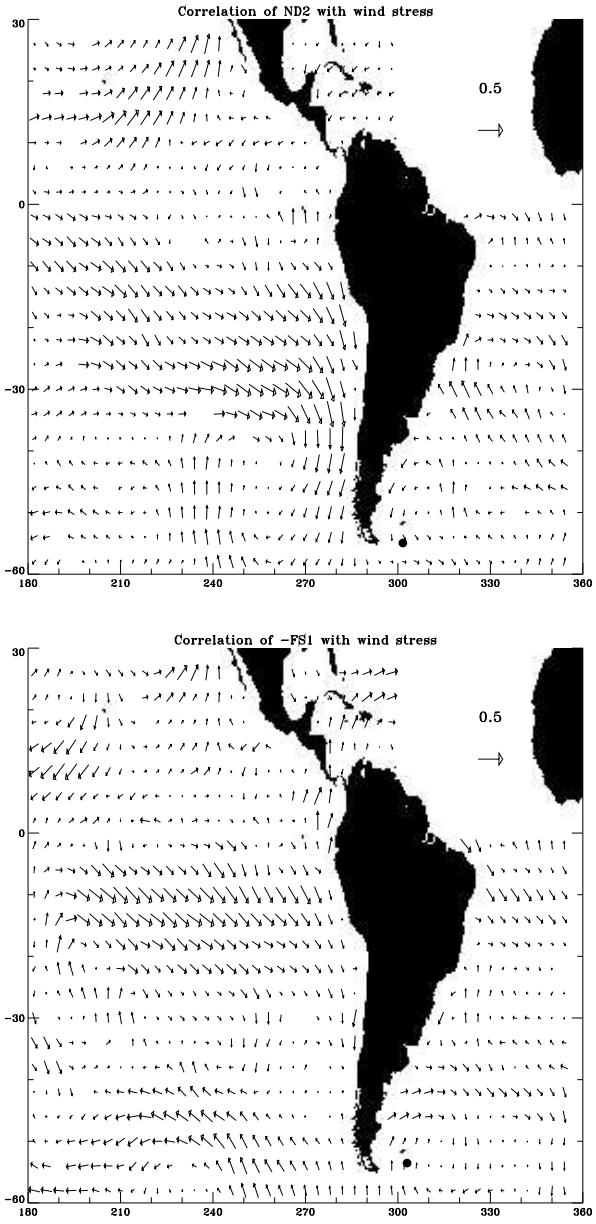

Figure 8. Vector correlation coefficients for NCEP reanalysis wind stress with in-situ bottom pressure measured at two sites to the north of Drake Passage, for periods of 30–170 days. The left panel has had the sign of the correlations reversed for comparison with the right panel. The black spot in each panel marks the position of the relevant instrument.

in this region are rather weak, and do not help to resolve the question. Indeed, the correlations shown here are mostly insignificant, as a Monte Carlo simulation suggests that a correlation of 0.32 is necessary for significance at the 95% confidence level, so we must appeal to the similarity in pattern as suggestive of the presence of a node between the two measurement depths. Simulaneous deployments at the two depths will be necessary to resolve this with any certainty.

4. Discussion

In oceans with vertical sidewalls, Kelvin waves are central to the theory of oceanic response to changes in wind stress and buoyancy (Wajsowicz and Gill, 1986; Kawase, 1987; Cane, 1989; Yang, 1999; Johnson and Marshall 2002a,b), permitting information to travel rapidly around the ocean boundaries and equator in comparison to the slower interior adjustment due to radiation of Rossby waves from the eastern boundary (Wajsowicz, 1986). In a realistic ocean, the various baroclinic Kelvin wave modes mutate into a hybrid Kelvin wave/barotropic continental shelf wave, the structure of which depends on the steepness of topography and the strength of stratification (Huthnance, 1978). The effect of these wave modes is to rapidly communicate information about changes in forcing along the continental slope.

Long-distance wave propagation was first clearly identified by Enfield and Allen (1980), using tide gauges along the eastern coast of North and South America. Reliable wave speeds are difficult to determine, but speeds are of the order of 1 ms^{-1}, and clearly poleward on this coast. The clearest effect of these waves in relatively low-frequency altimeter sampling is a strong correlation in SSP fluctuations along the continental shelf and slope. We have now identified similar long-distance correlations around the Antarctic, potentially in the Arctic, and along the North Pacific, North Atlantic, and South American continental slopes. The South American results in particular demonstrate correlations between eastern and western sides of the continent which are hard to explain as resulting from large-scale wind stress forcing (the opposite orientations of continental slopes on either side of the continent mean that a northward wind stress would produce responses of opposite signs on the two sides), strongly suggesting the influence of wave propagation on this signal. Wave propagation is particularly likely to be important in this region, since the Patagonian Shelf is wide, and wide shelves tend to result in more rapid wave propagation (eg. Hsueh (1980)).

Very little is known about the modal structure of these coherent signals, although theory suggests they are more likely to be baroclinic at low latitudes and barotropic at high latitudes. Results from north of Drake Passage suggest the dominant mode has a node somewhere between the 1000 m and 2800 m isobaths, but clear identification of the physical processes behind these correlations will require much more in-situ data, coupled with modelling studies. Given the fundamental nature of communication along the continental slope to theories of oceanic adjustment to changes in winds or thermohaline forcing, and the fact that these long-distance correlations seem to be quite common, we would suggest that a significant investment in modelling and further in-situ measurement of this phenomenon is warranted. In particular, measurements are required which can distinguish the different wave modes and their evolution along the slope, so that the observed structure of the coherent signal can be compared with calculated wave mode structure and full

three dimensional model predictions. This will be sufficient to test the hypothesis that the coherent signals are transmitted by coastal trapped waves, and to begin to assess the effect of friction over these long distances. Propagation of such waves has been suggested as a possible cause of observed differences between coastal and deep ocean sea level change (Holgate and Woodworth, 2004), as a means for coastal currents to extend far beyond the region of forcing (Huthnance, 1987), and as the mediator of the ocean's response to changes in deep convection (Johnson and Marshall, 2002, among others), so a more detailed understanding of their propagation and dissipation would be of interest for a wide range of oceanographic studies.

This work was funded by the U.K. Natural Environment Research Council as part of the Proudman Oceanographic Laboratory's Core Programme 1: Sea Level, Ocean Bottom Pressure, and Space Geodesy. The altimeter products were produced by the CLS Space Oceanography Division as part of the Environment and Climate EU ENACT project (EVK2-CT2001-00117) and with support from CNES.

References

Aoki, S., Coherent sea level response to the Antarctic Oscillation. *Geophys. Res. Lett., 29*, 10.1029/2002GL015733, 2002.

Cane, M. A., A mathematical note on Kawase's study of the deep-ocean circulation. *J. Phys. Oceanogr., 19*, 548–550, 1989.

Cartwright, D. E., J. M. Huthnance, R. Spencer, and J. M. Vassie, On the St Kilda shelf tidal regime. *Deep-Sea Res., 27A*, 61–70, 1980.

Chelton, D. B., and R. E. Davis, Monthly mean sea-level variability along the west coast of North America. *J. Phys. Oceanogr., 12*, 757–784, 1982.

Ducet, N., P.-Y. Le Traon, and G. Reverdin, Global high resolution mapping of ocean circulation from TOPEX/Poseidon and ERS-1/2. *J. Geophys. Res., 105*, 19477-19498, 2000.

Enfield, D. B., and J. S. Allen, On the structure and dynamics of monthly mean sea level anomalies along the Pacific coast of North and South America. *J. Phys. Oceanogr., 10*, 557–578, 1980.

Holgate, S. J., and P. L. Woodworth, Evidence for enhanced coastal sea level rise during the 1990s. *Geophys. Res. Letters, 31*, L07305, doi: 10.1029/2004GL019626, 2004.

Hsueh, Y., Scattering of continental shelf waves by longshore variations in bottom topography. *J. Geophys. Res., 85*, 1147–1150, 1980.

Hughes, C. W., and V. N. Stepanov, Ocean dynamics associated with rapid J2 fluctuations: Importance of circumpolar modes and identification of a coherent Arctic mode. *J. Geophys. Res. 109*, C06002, doi: 10.1029/2003JC002176, 2004.

Hughes, C. W., P. L. Woodworth, M. P. Meredith, V. Stepanov, T. Whitworth, and A. Pyne, Coherence of Antarctic sea levels, Southern hemisphere Annular Mode, and flow through Drake Passage. *Geophys. Res. Lett. 30*, 1464, doi: 10.1029/2003GL017240, 2003.

Hughes, C.W., M.P. Meredith and K. Heywood, Wind-Driven transport fluctuations through Drake Passage: A southern mode. *J. Phys. Oceanogr., 29*, 1971–1992, 1999.

Huthnance, J. M., On coastal trapped waves: Analysis and numerical calculation by inverse iteration. *J. Phys. Ocenogr., 8*, 74–92, 1978.

Huthnance, J. M., Along-shelf evolution and sea levels across the continental slope. *Cont. Shelf Res., 7*, 957–974, 1987.

Huthnance, J. M., Ocean-to-shelf signal transmission: A parameter study. *J. Geophys. Res., 109*, C12029, doi: 10.1029/2004JC002358, 2004.

Johnson H. L. and D. P. Marshall, A theory for the surface Atlantic response to thermohaline variability. *J. Phys. Oceanogr., 32*, 1121–1132, 2002a.

Johnson H. L. and D. P. Marshall, Localization of abrupt change in the North Atlantic thermohaline circulation. *Geophys. Res. Lett., 29*, 1083, 2002b.

Johnson M. A., A source of variability in Drake Passage. *Cont. Shelf Res., 10*, 629–638, 1990.

Kalnay, E., M. Kanamitsu, R. Kistler, W. Collins, D. Deaven, L. Gandin, M. Iredell, S. Saha, G. White, J. Woollen, Y. Zhu, M. Chelliah, W. Ebisuzaki, W. Higgins, J. Janowiak, K. C. Mo, C. Ropelewski, J. Wang, A. Leetmaa, R. Reynolds, R. Jenne, and D. Joseph, 1996, The NMC/NCAR 40-Year Reanalysis Project. *Bull. Amer. Meteor. Soc., 77*, 437–471, 1996.

Kawase, M., Establishment of deep ocean circulation driven by deep-water production. *J. Phys. Oceanogr., 17*, 2294–2317, 1987.

Meredith, M. P., P. L. Woodworth, C. W. Hughes, and V. Stepanov, Changes in the ocean transport through Drake Passage during the 1980s and 1990s, forced by changes in the Southern Annular Mode. *Geophys. Res. Lett.*, submitted, 2004.

Meredith, M. P., J. M. Vassie, K. J. Heywood, and R. Spencer, On the temporal variability of the transport through Drake Passage. *J. Geophys. Res., 101(C10)*, 22485-22494, 1996.

Meyers, S. D., A. Melsom, G. T. Mitchum, and J. J. O'Brien, Detection of the fast Kelvin wave teleconnection due to El Niño Southern Oscillation. *J. Geophys. Res., 103*, 27655-27663, 1998.

Orvik, K. A., and O. Skagseth, The impact of the wind stress curl in the North Atlantic on the Atlantic inflow to the Norwegian Sea toward the Arctic. *Geophys. Res. Lett., 30*, 1884, 2003.

Skagseth, O., Monthly to annual variability of the Norwegian Atlantic slope current: connection between the northern North Atlantic and the Norwegian Sea. *Deep-Sea Res., 51(3)*, 349-366, 2004.

Smith, W. H. F., and D. T. Sandwell, Global sea floor mapping from satellite altimetry and ship depth soundings. *Science, 277(5334),* 1956-1962, 1997.

Suginohara, N., Propagation of coastal-trapped waves at low latitudes in a stratified ocean with continental shelf slope. *J. Phys. Oceanogr., 11*, 1113–1122, 1981.

Vega, A., Y. du-Penhoat, B. Dewitte, and O. Pizarro, Equatorial forcing of interannual Rossby waves in the eastern South Pacific. *Geophys. Res. Lett., 30*, 1197, 2003.

Wajsowicz R. C. and A. E. Gill, Adjustment of the ocean under buoyancy forces .1. The role of Kelvin waves. *J. Phys. Oceanogr. 16(12)*, 2097–2114, 1986.

Wajsowicz R. C., Adjustment of the ocean under buoyancy forces .2. The role of planetary-waves. *J. Phys. Oceanogr. 16(12)*, 2115–2136, 1986.

Woodworth, P.L., J. M. Vassie, C. W. Hughes, and M. P. Meredith, A test of the ability of TOPEX/POSEIDON to monitor flows through the Drake Passage. *J. Geophys. Res., 101*, 11935–11947, 1996.

Woodworth, P. L., D. T. Pugh, M. P. Meredith and D. L. Blackman, Sea level changes at Port Stanley, Falkland Islands. *J. Geophys. Res.*, submitted, 2004.

Yang, Jiayan, A linkage between decadal climate variations in the Labrador Sea and the tropical Atlantic Ocean. *Geophys. Res. Lett., 26*, 1023-1026, 1999.